

## Accepted Manuscript

Carbohydrate-Supramolecular Gels: Adsorbents for Chromium(VI) Removal from Wastewater

Carla Rizzo, Jessica L. Andrews, Jonathan W. Steed, Francesca D'Anna

PII: S0021-9797(19)30456-4  
DOI: <https://doi.org/10.1016/j.jcis.2019.04.034>  
Reference: YJCIS 24863

To appear in: *Journal of Colloid and Interface Science*

Received Date: 6 March 2019  
Revised Date: 9 April 2019  
Accepted Date: 11 April 2019

Please cite this article as: C. Rizzo, J.L. Andrews, J.W. Steed, F. D'Anna, Carbohydrate-Supramolecular Gels: Adsorbents for Chromium(VI) Removal from Wastewater, *Journal of Colloid and Interface Science* (2019), doi: <https://doi.org/10.1016/j.jcis.2019.04.034>

This is a PDF file of an unedited manuscript that has been accepted for publication. As a service to our customers we are providing this early version of the manuscript. The manuscript will undergo copyediting, typesetting, and review of the resulting proof before it is published in its final form. Please note that during the production process errors may be discovered which could affect the content, and all legal disclaimers that apply to the journal pertain.



## Carbohydrate-Supramolecular Gels: Adsorbents for Chromium(VI) Removal from Wastewater

Carla Rizzo,<sup>a\*</sup> Jessica L. Andrews,<sup>b</sup> Jonathan W. Steed<sup>b</sup> and Francesca D'Anna<sup>a\*</sup>

<sup>a</sup>Università degli Studi di Palermo, Dipartimento di Scienze e Tecnologie Biologiche Chimiche e Farmaceutiche, Viale delle Scienze, Ed. 17, 90128, Palermo (Italia).

<sup>b</sup>Department of Chemistry, Durham University, South Road, Durham, DH1 3LE, UK.

\*email corresponding author: francesca.danna@unipa.it; carla.rizzo03@unipa.it

### Abstract

*Hypothesis.* To overcome the contamination of water by heavy metals the adsorption of the pollutant on gel phases is an attractive solution since gels are inexpensive, potentially highly efficient and form a distinct phase while allowing diffusion of the contaminated water throughout the material. This work tests the chromium(VI) adsorbent capacity of new supramolecular gels for Chromium(VI) removal from wastewater.

*Experiments.* First hydrophobic imidazolium salts of carbohydrate anions were synthesised as new gelators. Subsequently, they were dissolved in a solvent by heating and, after cooling overnight, to give the formation of supramolecular gels. The properties of the resulting gels, such as thermal stability, mechanical strength, morphology, rheology, and kinetics of gel formation, were studied as a function of gelator structure, gelation solvent and pollutant removal efficiency.

*Findings.* Carbohydrate-derived gels showed the best removal capacity, *i.e.* 97% in 24 h. Interestingly, in one case, the reduction of chromium(VI) to chromium(III) also occurred after the adsorption process, and this phenomenon has been analysed using <sup>1</sup>H NMR spectroscopy, IR spectroscopy, and SEM. The most efficient gel can reach an adsorption capacity of 598 mg/g in contrast to a value of 153 mg/g for the most effectively best hydrogels reported to date. The new gel can be also recycled up to 4 times. These findings suggest that these new, supramolecular hydrogels have potential applications in environmental remediation.

**Keywords.** Supramolecular gels, carbohydrates gelators, hexavalent chromium, reduction of toxic metal, chemisorption, environmental remediation, wastewater treatment.

## 1. Introduction

Water pollution due to the release of hazardous waste such as heavy metals, dyes, pharmaceuticals, petroleum products, pesticides, and fertilisers into the environment is a serious concern in modern society.[1] Hexavalent chromium (Cr(VI)) is one of the most toxic heavy metal pollutants and arises from several industrial processes.[2] Cr(VI) can easily be absorbed by the skin causing arthritis, bronchitis, nerve damage, brain damage, and cancer.[3] Due to the high solubility of Cr(VI) in water, its accumulation into natural aquatic environments is common.[4] Therefore, the search for new materials able to “catch” Cr(VI) and to clean water is quite urgent.

Several methods have been used to remove heavy metal ions from wastewater, for example, chemical precipitation, ion-exchange, adsorption, membrane filtration and electrochemical treatment.[5] Whilst all methods have pros and cons, adsorption processes offer the desirable combination of being both effective and cost-efficient. Indeed, adsorption methods offer flexibility in the design of specialised sorbents and facilitate cleaning operations which produce high-quality treated effluent. In addition, if the adsorption process is reversible, the adsorbent can be regenerated by a suitable desorption process.[5] Many adsorbents have been developed to eliminate Cr(VI) from wastewater, in particular, activated carbons,[6] zeolites,[7] clays,[8] nanomagnetic particles,[9, 10] photocatalytic nanocomposites,[11] biosorbents[12] and silica materials.[13] However, some of these materials are expensive and difficult to dispose of after use. In addition, they can suffer from low adsorption capacity and selectivity, due to a low porosity and surface area, or the lack of necessary functional groups.

The use of soft materials like gels can be a valid alternative, as they can overcome all these problems. Recently, polymeric and hybrid gels have been used to remove Cr(VI) from aqueous solution. For example, a redox-responsive copper(I) metallogel,[14] a sponge-like porous composite chitosan hydrogel formed with reduced graphene oxide and montmorillonite[15] and a porous 3D folic acid-polyaniline hybrid hydrogel[16] have been reported. In all cases, high efficiency was observed, especially in acidic conditions.

Supramolecular gels have recently been applied for the adsorption of heavy metals and dyes,[17, 18] but they have rarely been used for the selective removal of Cr(VI). Supramolecular gels are soft materials formed by low molecular weight molecules that can self-assemble through supramolecular interactions and immobilise the surrounding solvent by surface tension.[19, 20] The self-aggregation of the small gelator molecules through a combination of non-covalent interactions such as hydrogen bonding,  $\pi$ - $\pi$  stacking, donor-acceptor interactions, metal coordination and van der Waals forces results in an entangled self-assembled fibrillar network. Since these networks

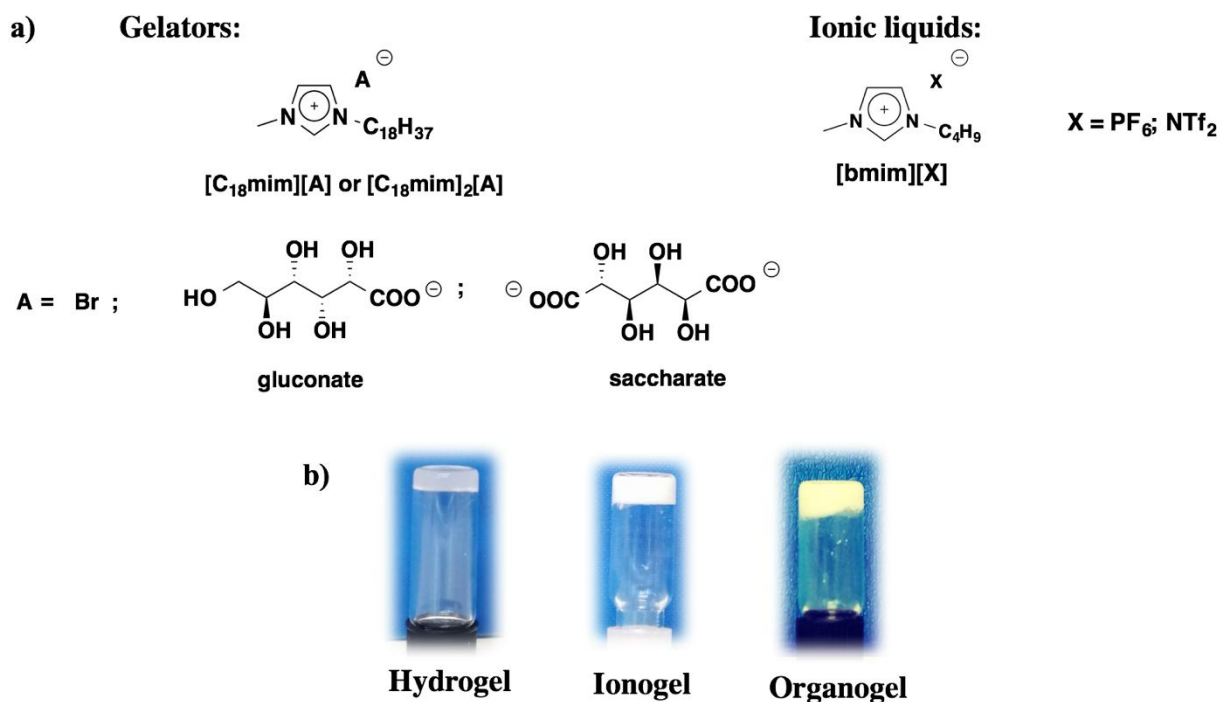
involve weak interactions, they can be readily transformed to a fluid by heating and are generally reversible.[21] For this reason, these materials can be considered “smart” as they can selectively respond to external stimuli such as temperature, ultrasound, light, *pH* and mechanical disruption.[22]

Depending on the nature of the solvent, a gel can be classified as an organo-, hydro-, or ionogel. The term ‘ionogel’ refers to a wide range of materials including polymeric, silica and a few examples of supramolecular gels, in which the solvent is an ionic liquid (IL). Ionic liquids are organic salts with a melting temperature below 100 °C and have been used in recent times as “green solvents”, by virtue of their low flammability and volatility.[23-25] Usually, the formation of an ionogel can enhance the properties of the parent IL. In addition to the absence of volatility and flammability of the IL, ionogels can be more conductive and thermally stable.[26-28] Similarly, the structural versatility of ionogels allows their application in various fields, including bio-medicine,[29] as anti-oxidants,[30] in environmental remediation[31-33] and in catalysis.[34]

Herein we propose the use of easily synthesisable organic salts as gelators.[35] They are formed by combining the 1-methyl-3-octadecyl imidazolium cation [**C<sub>18</sub>mim**<sup>+</sup>] with a range of mono- and dianions, that differ in nature, size and coordination ability, *i.e.* bromide [**Br**<sup>-</sup>], gluconate and saccharate anions (Scheme 1a).

Particular attention has recently been devoted to carbohydrate-derived gelators, thanks to their biodegradability and non-toxicity. In addition, these gelators can be formed from cheap and renewable starting materials.[36] The main driving force for gel formation in carbohydrate-based gelators is intermolecular hydrogen bonding between the hydroxyl groups on the gelator and solvent molecules. However, the inclusion of aromatic or hydrophobic functional groups that facilitate the formation of  $\pi$ - $\pi$  stacking or van der Waals interactions is necessary to give a powerful gelator.[37] In this work, we report imidazolium salts of carbohydrate derived gelators. The imidazolium cation bearing a long alkyl chain represents a hydrophobic counter cation to the hydrophilic, carbohydrate-derived anions. Furthermore, given that a different stoichiometry between the cation and anion of the gelator can influence the gel properties,[38] we have also synthesised a gelator formed from monocationic imidazolium and dianionic units: [**C<sub>18</sub>mim**]<sub>2</sub>[**saccharate**].

The gelling ability of new organic salts was tested in a wide range of solvents, spanning from water to organic solvents and ILs. The chosen ILs were composed of the most commonly used 1-methyl-3-butyl imidazolium [**bmim**<sup>+</sup>] monocation, with anions presenting different coordination abilities, including (hexafluorophosphate [**PF<sub>6</sub>**<sup>-</sup>] and *N,N*-bis(trifluoromethanesulfonyl)imide [**NTf<sub>2</sub>**]) (Scheme 1a).



**Scheme 1.** a) Structure of gelators and ILs used to form gels; b) photos of hydrogel, ionogel and organogel formed by  $[C_{18}mim][Br]$  in water,  $[bmim][PF_6]$  and diesel fuel, respectively.

During gelation tests, the tube-inversion method was used to qualitatively identify the formation of a supramolecular gel. The thermal behaviour of the gels and gelators was analysed using Differential Scanning Calorimetry (DSC). Rheological techniques were used to quantitatively investigate the physical nature of the gel phases, and their morphology was analysed using Polarizing Optical Microscopy (POM) and Scanning Electron Microscopy (SEM). Furthermore, the kinetics of gel formation were measured using UV-visible spectroscopy.

The fully characterized gels were then applied to water treatment. In particular, metal adsorption experiments were carried out on several gels, and for the best systems, the kinetics of adsorption were investigated. Interestingly, our gels selectively adsorb Cr(VI) and in one case, its reduction to Cr(III) was observed. To ensure that the reduction process had occurred, a range of experiments were undertaken, including  $^1H$  NMR spectroscopy, IR spectroscopy, and SEM. These carbohydrate derived gels stand out for use in the treatment of Cr(VI)-contaminated water because they are able to adsorb the metal, and then also convert it to a less toxic species.

## 2. Materials and methods

2.1. *Materials.* 1-methylimidazole, octadecane bromide, D-gluconate potassium salt, D-saccharic acid potassium salt, Amberlite resin IR 120 PLUS, Amberlite resin IRA-400, sodium hydroxide, hydrochloric acid at 37 wt %, potassium bichromate, Alizarin Red S (3,4-dihydroxy-9,10-dioxo-2-anthracenesulfonic acid sodium salt), sodium tetraborate, copper(II) nitrate hemi(pentahydrate), cobalt(II) nitrate hexahydrate, zinc(II) nitrate monohydrate, nickel(II) nitrate hexahydrate and all organic solvents used were analytical reagents purchased from commercial sources and used as received.

ILs, such as [bmim][NTf<sub>2</sub>] and [bmim][PF<sub>6</sub>], were analytical reagents purchased from commercial sources and used as received.

All water buffers were prepared with ultra-pure millipore water ensuring that the pH value was equal to 7.4 with a common pH meter. Synthetic sea water (SW) was prepared in agreement with Italian analytical methodologies to accept suitable adsorbents for water treatment.[39]

2.2. *Methods.* The new gelators synthesised were characterised by <sup>1</sup>H, <sup>13</sup>C NMR, ESI-MS spectroscopy and elemental analysis. The NMR spectra were recorded by using Bruker 300 MHz or 400 MHz Bruker Avance III nuclear magnetic resonance spectrometers. Electrospray-ionisation mass spectra of gelators were obtained from dilute (1 mg mL<sup>-1</sup>) samples in methanol using a TQD mass spectrometer (Waters Ltd.). Elemental analysis was carried out on dried materials using an Exeter CE-440 Elemental Analyser.

*DSC measurements.* DSC was carried out on a DSC Q20 calorimeter (TA Instruments) interfaced to a TA thermal analyst 2000 controller connected to a RCS90 cooling system and on a Perkin Elmer Pyris 1 DSC. Heating and cooling cycles were done in a 50 mL min<sup>-1</sup> stream of nitrogen.

The samples were weighed (5 mg for salts, 15 mg for gels) in Tzero aluminium pans. The transition temperatures from the DSC measurements are reported at the point of maximum heat flow.

After equilibration of the sample at 25 °C, DSC measurements of the organic salts were performed by heating the sample with rates of 10 °C min<sup>-1</sup> from 25 to 110 or 140 °C and cooling it with the same rate ramp to 0 °C. DSC measurements of the gel phases were performed by equilibrating the sample at -10 °C for 2 min and by using a temperature ramp with a rate of 5 °C min<sup>-1</sup> from -10 to 75 °C and a cooling ramp to -10 °C.

The melting temperatures and crystallisation temperatures ( $T_m$  and  $T_c$ , respectively) and the enthalpy change corresponding to the melting or crystallisation processes ( $\Delta H_m$  and  $\Delta H_c$ ,

respectively) were determined at the maximum of the heat flows in the DSC thermograms and as the integrated areas of the melting calorimetric peaks, respectively. All measurements were repeated twice to assure their reproducibility.

*POM measurements.* Gels at 5 wt% of the gelator were casted between two glasses to record the POM images. The samples were heated to their sol phases and cooled. The instrument used was an Olympus BX53 microscope equipped with crossed polarisers, a Linkam hotstage, an Olympus XC50 camera interfaced to a computer with Steambasic Software and a Linkam microprocessor thermometer connected to a K thermocouple.

*Scanning electron microscopy.* SEM samples were prepared on silicon wafers, dried in air for 2 days, and coated with 2 nm of platinum using a Cressington 328 Ultra High Resolution EM Coating System. The images were obtained using an FEI Helios NanoLab DualBeam microscope in immersion mode, with beam settings of 1.5 kV and 0.17 nA.

*Opacity measurements.* Opacity measurements were recorded with a spectrophotometer Beckman Coulter DU 800. The opacity of the gel phases was determined with UV/Vis measurements as a function of time, at a wavelength of 568 nm and a temperature of 25 °C. Samples for a typical measurement were prepared by injecting into a quartz cuvette (light path 0.2 cm) a hot solution of the salt. Spectra were recorded until gel formation. The gel phase obtained at the end of the measurement was stable according to the tube inversion test.

*IR spectra.* IR spectra of xerogels and powders were recorded on Perkin Elmer Spectrum 100 Universal ATR instrument.

**2.3. Synthesis of bromide salt [C<sub>18</sub>mim][Br].** Imidazolium salts were synthesized modifying a previously reported procedure.[40] To an acetonitrile solution of 1-methylimidazole (2 g, 0.024 mol in 100 mL) was added dropwise a solution of octadecane bromide (4.7 g, 0.024 mol in 200 mL). The mixture was stirred at 90 °C for 48 h under an Ar atmosphere. The reaction solvent was evaporated under vacuum and a brown waxy solid was obtained. This residue was washed using petroleum ether (3 x 75 mL) with the aid of ultrasound irradiation and a white solid was obtained.

Finally, to a solution of the desired product in  $\text{CH}_2\text{Cl}_2$  was added 1 wt % of charcoal at 0 °C and the mixture was stirred overnight. Then the solution was filtrated under vacuum with a Gooch funnel and the evaporation of the filtrate gave rise to a white powder.

Yield = 74 %; m.p. = 62.7 °C.  $^1\text{H-NMR}$  (300 MHz)  $\text{CDCl}_3$  ( $d_1$ ),  $\delta$  (ppm): 0.86 (t,  $J = 6$  Hz, 3H), 1.28 (m, 30H), 1.90 (m, 2H), 4.12 (s, 3H), 4.30 (t,  $J = 6$  Hz, 2H), 7.29 (s, 1H), 7.41 (s, 1H), 10.54 (s, 1H).  $^{13}\text{C-NMR}$  (300 MHz)  $\text{CDCl}_3$  ( $d_1$ ),  $\delta$  (ppm): 14.1, 22.6, 26.2, 29.0, 29.3, 29.4, 29.5, 29.6, 29.7, 29.8, 30.3, 31.9, 50.2, 121.8, 123.6, 137.5. ESI (m/z): 336 [(M-A) +  $\text{H}$ ] $^+$ ; 115 [M- C + Cl] $^-$ . Elemental Anal. Calcd. for  $\text{C}_{22}\text{H}_{43}\text{BrN}_2$  (414.5): C, 63.60; H, 10.43; N, 6.74. Found: C, 63.41; H, 10.47; N, 6.72.

**2.4. Anion exchange procedure.** The acid form of the desired carbohydrate-anion was obtained from the corresponding potassium salt utilizing the acid resin IR 120 PLUS (3.5 g for 0.0004 mol of salt). The resin was charged with an aqueous solution of HCl (20 mL, 10% v/v); the excess of the HCl solution was removed by washing the resin with water until neutrality of pH. Then a water solution of the desired potassium salt was eluted through the resin to obtain the corresponding acid.

When the acid was obtained, the anion exchange was carried out as previously reported. A column packed with anion-exchange Amberlite resin IRA-400 (chloride form) (2.5 g) was used. To convert the chloride form of the resin into the hydroxide form, the column was first washed with an aqueous solution of NaOH (10 mL, 10% w/v) and subsequently with water until the eluate was pH neutral. A binary mixture of methanol/water (70/30, v/v) was used as eluent. The bromide salt (4.72 g, 6.21 mmol) was dissolved in the binary solvent mixture (50 mL) and eluted. The eluate was collected in a flask containing a solution of the corresponding acid in a stoichiometric amount. The neutral solution was concentrated in *vacuo* and the residue was washed with hexane while being subjected to ultrasound (3x100 mL).

**[C<sub>18</sub>mim][gluconate]:** Yield = 93 %; white powder; m.p. = 57.2 °C.  $^1\text{H-NMR}$  (300 MHz)  $\text{CDCl}_3$  ( $d_1$ ),  $\delta$  (ppm): 0.87 (t,  $J = 6$  Hz, 3H), 1.25 (m, 30H), 1.81 (m, 2H), 3.53 (m, 1H), 3.65 (m, 3 H), 3.97 (s, 4H), 4.06 (s, 1H), 4.21 (t,  $J = 6$  Hz, 2H), 7.46 (s, 1H), 9.59 (s, 1H).  $^{13}\text{C-NMR}$  (300 MHz)  $\text{CDCl}_3$  ( $d_1$ ),  $\delta$  (ppm): 14.1, 22.7, 26.4, 29.2, 29.4, 29.5, 29.7, 29.8, 29.9, 30.3, 31.9, 36.7, 49.8, 63.6, 63.9, 121.4, 123.8, 137.2, 177.4. ESI (m/z): 336 [(M-A) +  $\text{H}$ ] $^+$ ; 194 [M-C - H] $^-$ . Elemental Anal. Calcd. for  $\text{C}_{28}\text{H}_{54}\text{N}_2\text{O}_7$  (530.9): C, 63.37; H, 10.26; N, 5.28. Found: C, 63.15; H, 10.29; N, 5.26.

**[C<sub>18</sub>mim]<sub>2</sub>[saccharate]**: Yield = 95 %; waxy white solid; m.p. = 56.4 °C. <sup>1</sup>H-NMR (300 MHz) CDCl<sub>3</sub> (d<sub>1</sub>), δ (ppm): 0.87 (t, J = 6 Hz, 6H), 1.24 (m, 60H), 1.83 (m, 4H), 3.91 (m, 2H), 4.00 (s, 6 H), 4.03 (m, 1H), 4.12 (m, 1H), 4.24 (t, J = 6 Hz, 4H), 7.19 (s, 2H), 7.33 (s, 2H), 9.87 (s, 2H). <sup>13</sup>C-NMR (300 MHz) CDCl<sub>3</sub> (d<sub>1</sub>), δ (ppm): 14.1, 22.4, 26.3, 29.1, 29.4, 29.5, 29.6, 29.7, 29.8, 30.3, 31.9, 36.2, 49.9, 71.8, 73.6, 75.4, 121.1, 123.4, 138.1. ESI (m/z): 336 [(M-A)/2 + H]<sup>+</sup>; 207 [M-C - H]<sup>-</sup>. Elemental Anal. Calcd. for C<sub>50</sub>H<sub>94</sub>N<sub>4</sub>O<sub>8</sub> (879.7): C, 68.30; H, 10.78; N, 6.37. Found: C, 68.47; H, 10.74; N, 6.39.

**2.5. Preparation of the gels and determination of  $T_{gel}$ .** The gels were prepared by weighing into a screw-capped sample vial (diameter 1 cm) the amount of imidazolium salt, previously synthesised as described above, and the corresponding solvent ( $\approx$  250 mg). The mixture was first dispersed for five minutes with ultrasound irradiation and subsequently heated in an oil bath to 80 °C until a clear solution was obtained.[21] The vial was then cooled and stored overnight at room temperature. The tube inversion test method was used to examine gel formation.[41]

$T_{gel}$  was determined by the falling-drop method.[42] The vial containing the gel was immersed, turned upside down in a water bath, the bath temperature was gradually increased (2 °C min<sup>-1</sup>) until the first drop of the gel fell. The  $T_{gel}$  values were reproducible within 1 °C.

**2.6. Rheological measurements.** Rheology measurements were recorded at room temperature on a TA Instruments AR 2000 equipped with a rough Peltier plate with 25 mm rough plate geometry. Samples were prepared by heating mixtures of gelator and solvents in sealed vials. The hot solutions, then, were poured into a 25 mm cylindrical glass mould on the Peltier plate and the gels allowed to form over 30 minutes prior to analysis. The materials were cooled to 25 °C throughout formation and analysis. Rheological properties, such as the stress sweep and the frequency sweep, were recorded three times on three different aliquots of the gels.

**2.7. Thixotropic and sonotropic behaviour.** The gel phases obtained were subjected to two different external stimuli. The mechanical stimulus involved stirring the gel phase at 1000 rpm for 5 min by using a stirrer bar (length = 8 mm, height = 3 mm). The sonotropic behaviour of the gel phases was tested by irradiating in an ultrasound water bath for 5 min with a power of 200 W and a frequency of 45 kHz. Thereafter, the materials were stored at room temperature overnight. When the samples were stable to the tube inversion test, the gels were defined as thixotropic or sonotropic, respectively.

2.8. *Metal adsorption.* The removal efficiency (RE) of metals from aqueous solution was estimated using UV/vis spectroscopy with a Cary series UV-vis-NIR 5000 Agilent Technologies spectrophotometer. The final concentration of the metal in solution was calculated according to the Beer–Lambert law ( $A = \epsilon bc$ ; where  $A$  is the absorbance of the metal,  $\epsilon$  is the molar extinction coefficient in units of  $\text{mol L}^{-1} \text{cm}^{-1}$ ,  $b$  is the path length of the incident light with the units  $\text{cm}$ ,  $c$  is the concentration of the metal in solution with the units  $\text{mol L}^{-1}$ ). The molar extinction coefficient of Chromium (VI) ( $A_{350 \text{ nm}}$ ) in aqueous solution was equal to  $3011.15 \text{ mol L}^{-1} \text{cm}^{-1}$  with  $b = 0.2 \text{ cm}$ , and the final concentration of the metal in solution was obtained by the Beer–Lambert equation. Finally, the removal efficiency of the gel was obtained as reported in equation (1):

$$\text{RE} = (C_i - C_f)/C_i \quad (1)$$

in which  $C_i$  represents the initial concentration of the metal in solution;  $C_f$  is the final concentration of the metal in the presence of an adsorbing agent.

The removal of metal solutions was firstly tested in vials; in particular,  $300 \mu\text{L}$  of a water solution of Chromium (VI) ( $1.7 \cdot 10^{-3} \text{ M}$ ) or divalent metal ( $2.6 \cdot 10^{-3} \text{ M}$ ) were casted on the top of  $250 \text{ mg}$  of gels at  $5 \text{ wt } \%$ .

The adsorption capacity of gels was also investigated in batch experiments where  $250 \text{ mg}$  or  $20 \text{ mg}$  of gel at  $5 \text{ wt } \%$  of gelator were immersed in chromium solutions of  $10$  or  $20 \text{ mL}$  volume respectively, according to eq 2:

$$q_e = \frac{(C_o - C_e) \cdot V}{m} \quad (2)$$

where  $q_e$  is the adsorption capacity ( $\text{mg/g}$ ),  $C_o$  and  $C_e$  are the initial ( $500 \text{ mg/L}$ ) and equilibrium concentration of the adsorbate in the solution phase ( $\text{mg/L}$ ), respectively,  $V$  is the solution volume ( $\text{L}$ ), and  $m$  is the hydrogelator mass ( $\text{g}$ ).[43]

Recycle of the adsorbing gel was carried out by loading the suitable gel with the  $\text{K}_2\text{Cr}_2\text{O}_7$  water solution as previously described. After  $24 \text{ h}$ , the decolorized aqueous solution was removed and replaced with a fresh batch of  $300 \mu\text{L}$  of a  $1.7 \cdot 10^{-3} \text{ M}$  of  $\text{K}_2\text{Cr}_2\text{O}_7$  solution in water. After each cycle, the gel maintained its characteristics as evidenced by the tube inversion test.

2.9. *Kinetics of Chromium (VI) adsorption.* The time of removal efficiency of gels was tested with a kinetics experiment, in which  $300 \mu\text{L}$  of Chromium (VI) water solution ( $1.7 \cdot 10^{-3} \text{ M}$ )

were casted on the top of 250 mg of gels at 5 wt %. In particular, kinetics experiments were performed in batch, using different gels for each point of the kinetic curve. At fixed intervals of time ( $\approx 0.25, 0.50, 0.75, 1, 2, 3, 4, 5, 6, 18, 24$  and  $30$  h),  $250 \mu\text{L}$  of supernatant solutions were removed to be spectrophotometrically analysed by monitoring the chromium(VI) peak at  $350$  nm. The concentration of chromium(VI) was determined with a calibration curve. The same experiment was carried out with the IL used as gelation solvent as blank for ionogel phases.

- 2.10.  *$^1\text{H}$  NMR analysis to test gel component release.*  $300 \mu\text{L}$  of  $\text{D}_2\text{O}$  were casted on  $250$  mg of gel (hydrogels in SW were prepared using  $\text{D}_2\text{O}$ ), after  $24$  h the supernatant solution was analysed *via*  $^1\text{H}$  NMR. The  $^1\text{H}$  NMR spectra were recorded by using 5-hydroxymethylfurfural as reference compound. The reference signals did not superimpose with those of the gelators or IL, so it was possible to determine the amount of component release by comparing peak areas of reference and gel components.
- 2.11. *Divalent metal adsorption.* Due to the low molar extinction coefficient of divalent metals, it was not possible to estimate directly the metal concentration through UV-vis measurements. So,  $200 \mu\text{L}$  of divalent metal solution ( $2.6 \cdot 10^{-3}$  M) was reacted with  $200 \mu\text{L}$  of tetraborate ( $0.02$  M) buffer solution of Red Alizarin S ( $1.3 \cdot 10^{-3}$  M) to form a complex with different absorption bands from pure Alizarin Red S buffer solution.[44] The pure spectrum of Alizarin Red S buffer presents two main absorption bands at  $254$  and  $452$  nm, those bands bathochromically shifted in presence of divalent metals to a range of  $259$ - $268$  nm and  $518$ - $550$  nm depending on the metal selected.

### 3. Results and Discussion

DSC analysis revealed that all the imidazolium salts synthesised in this work behaved as ILs, presenting a melting temperature below  $100$  °C; for this reason, they can be defined as ionic liquid gelators. Table 1 summarises the results obtained, and DSC traces are reported in Figure S1.

**Table 1.** Melting temperature ( $T_m$ ), enthalpy change corresponding to the melting transition ( $\Delta H_m$ ), crystallization temperature ( $T_c$ ), enthalpy change corresponding to the crystallization transition ( $\Delta H_c$ ).

Gelators	$T_m$ (°C)	$\Delta H_m$ (J/g)	$T_c$ (°C)	$\Delta H_c$ (J/g)
[C <sub>18</sub> mim][Br]	62.8	79.7	49.4	58.3
	70.1 <sup>a</sup>	5.2 <sup>a</sup>		
	55.8 <sup>b</sup>	55.4 <sup>b</sup>	49.5 <sup>b</sup>	55.3 <sup>b</sup>
[C <sub>18</sub> mim][gluconate]	57.2	78.6	41.1	59.9
	50.8 <sup>b</sup>	58.1 <sup>b</sup>	41.4 <sup>b</sup>	58.6 <sup>b</sup>
[C <sub>18</sub> mim] <sub>2</sub> [saccharate]	54.3 <sup>c</sup>	48.4	50.9	49.7

<sup>a</sup>second transition, <sup>b</sup>second heating and cooling cycle, <sup>c</sup>first and second heating and cooling cycle matched completely.

The main difference in the thermal behaviour of these gelators is that two main transitions were observed during the heating cycle of the bromide salt, whereas only one transition was observed for the two carbohydrate-derived gelators based on gluconate and saccharate. In addition, the carbohydrate-derived anions seem to impart a lower degree of crystallinity to the salt, as these materials melt at a lower temperature and, in the case of saccharate salt, with a lower enthalpy ( $\Delta H_m$ ). In general, the melting temperature ( $T_m$ ) varied as follows: [C<sub>18</sub>mim][Br] > [C<sub>18</sub>mim][gluconate] > [C<sub>18</sub>mim]<sub>2</sub>[saccharate].

$T_m$  does not vary significantly between the carbohydrate-derived monoanion and dianion gelators; however, the enthalpy change is significantly decreased. This difference is also evident by looking at the enthalpy variation of the crystallisation process. It is likely that the presence of two cations and one dianion caused the formation of a less closely packed structure in this case.

The higher degree of crystallinity of the bromide salt, with respect to the carbohydrates, is also shown by its better gelling ability. This compound has a lower critical gelation concentration (CGC) than the others and also gels a larger number of solvents (Table 2 and S1). Gels were prepared by dissolving the imidazolium salts in the relevant solvent by heating and cooling it overnight. All the gels formed were stable to the tube inversion test at room temperature for more than 4 months (Scheme 1b).[41]

**Table 2.** Critical gelation concentration (CGC),  $T_{gel}$  at CGC and  $T_{gel}$  at 5 wt %.

Solvent	[C <sub>18</sub> mim][Br]			[C <sub>18</sub> mim][gluconate]			[C <sub>18</sub> mim] <sub>2</sub> [saccharate]		
	CGC (wt%) <sup>a</sup>	$T_{gel}$ (°C) <sup>b</sup>	$T_{gel}$ (°C)	CGC (wt%) <sup>a</sup>	$T_{gel}$ (°C) <sup>b</sup>	$T_{gel}$ (°C)	CGC (wt%) <sup>a</sup>	$T_{gel}$ (°C) <sup>b</sup>	$T_{gel}$ (°C)
water	1.0	14	22 <sup>d</sup>	-			-		

			40 <sup>e</sup>						
PB	0.7	19	39 <sup>d</sup>	-			-		
			43 <sup>e</sup>						
PBS (1x)	0.5	SM <sup>c</sup>	39 <sup>d</sup>	4.6	28	29 <sup>d</sup>	1.0	SM	32 <sup>d</sup>
			41 <sup>e</sup>			31 <sup>e</sup>			34 <sup>e</sup>
NaCl water solution (20 mM)	0.5	SM <sup>c</sup>	40 <sup>d</sup>	-			-		
			40 <sup>e</sup>						
SW	1.0	35	42 <sup>d</sup>	2.0	18	35 <sup>d</sup>	3.8	39	32 <sup>d</sup>
			41 <sup>e</sup>			38 <sup>e</sup>			38 <sup>e</sup>
Diesel	5.5	27	27 <sup>d</sup>	-			-		
			60 <sup>e</sup>						
[bmim][PF <sub>6</sub> ]	1.0	35	62 <sup>d</sup>	0.8	32	54 <sup>d</sup>	0.5	27	61 <sup>d</sup>
			63 <sup>e</sup>			58 <sup>e</sup>			65 <sup>e</sup>
[bmim][NTf <sub>2</sub> ]	3.1	33	36 <sup>d</sup>	1.0	17	27 <sup>d</sup>	4.7	32	38 <sup>d</sup>
			36 <sup>e</sup>			29 <sup>e</sup>			42 <sup>e</sup>

<sup>a</sup> values corresponding to the critical gelation concentration (CGC), concentration in % w/w (g/g); <sup>b</sup>  $T_{gel}$  at CGC determined with the falling drop method, reproducible within 1 °C; <sup>c</sup> SM = soft material (it was not possible to observe the falling of the first drop of gel and determine the  $T_{gel}$ ); <sup>d</sup>  $T_{gel}$  at 5 wt % determined with falling drop method, reproducible within 1 °C; <sup>e</sup>  $T_{gel}$  at 5 wt % determined with DSC measurements.

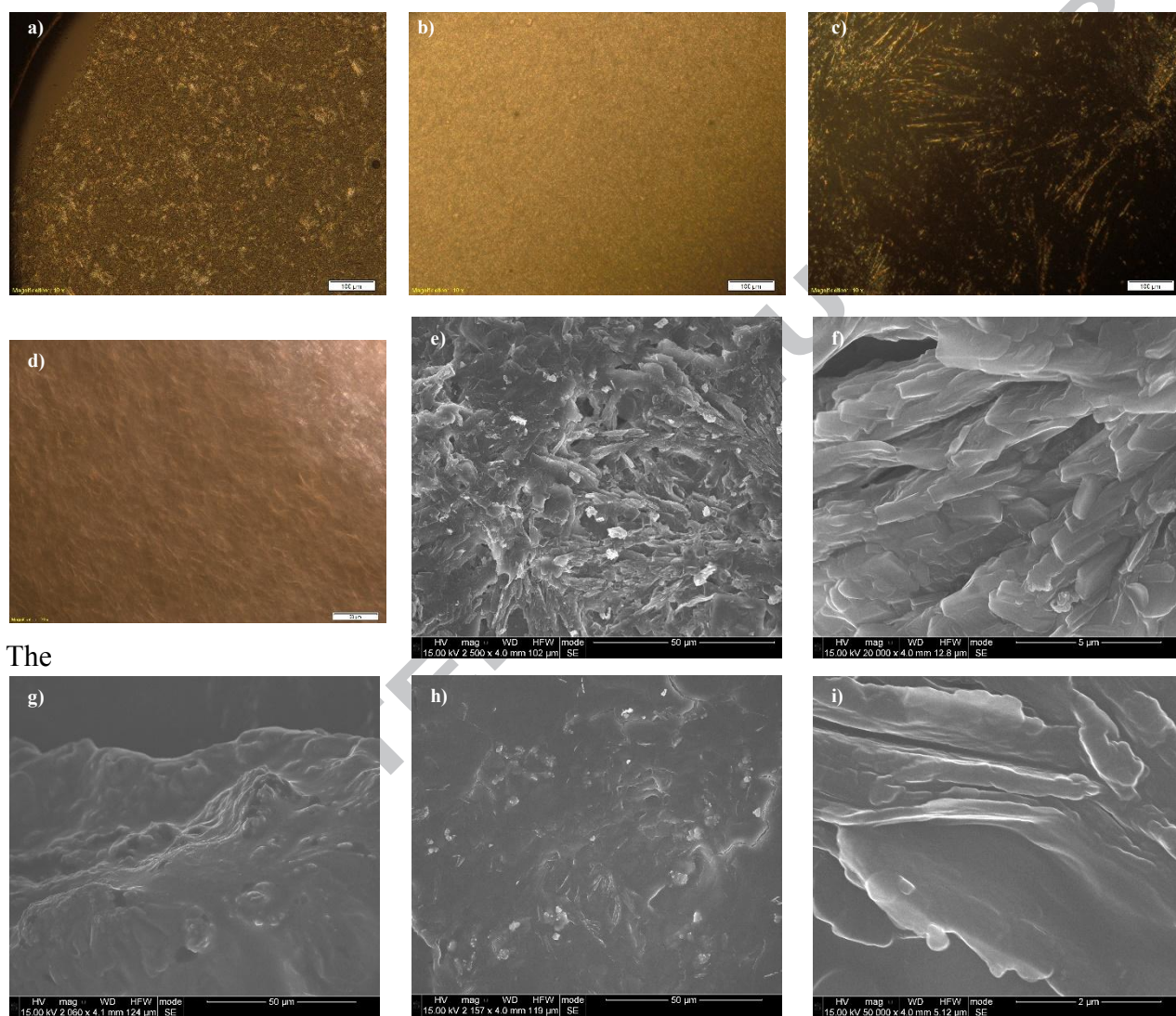
Interestingly, all gelators were able to gel water solutions and ILs, but **[C<sub>18</sub>mim][Br]** was the only one which also gelled diesel fuel. Gelation of oils has been reported as a new alternative for oil spill recovery from water.[45-47] In light of this, **[C<sub>18</sub>mim][Br]** is a versatile gelator that could be potentially used for several environmental applications. In addition, it was able to gel water solutions irrespective of their ionic strength, including water, phosphate buffer (PB), phosphate buffer saline solution (1x) [PBS (1x)], NaCl water solution and seawater (SW). Conversely, the carbohydrate salts preferentially gelled solutions with a higher ionic strength such as PBS (1x) and SW.

Interestingly, DSC analysis (Figure S2) revealed multiple transitions in the melting process for some gels, indicating a partial rearrangement of the gel network before the complete melting. However, these small melting transitions are not detected either with the falling drop method or with hot stage POM, so they cannot be ascribed to a macroscopic morphological change in the gel network.

In general, the anion had a significant effect on gelation; in particular, gels of **[C<sub>18</sub>mim][Br]** presented a higher  $T_{gel}$ , at same gelator concentration, than the carbohydrate analogues. Between the carbohydrate-based gelators,  $T_{gel}$  at 5 wt % was higher for **[C<sub>18</sub>mim]<sub>2</sub>[saccharate]** gels than for **[C<sub>18</sub>mim][gluconate]**. The different thermal behaviour observed in solution and in the bulk solids (see above) may be due to the presence of multiple interactions of the dianionic salt that in solution might favour gel formation. A similar trend was previously observed for some anion dipeptide based gelators.[29]

The thermal stability of the gels is also heavily affected by solvent nature. As expected, ionogels display a higher thermal stability than the analogous hydrogels, when an IL with a high cross-linking ability, such as [bmim][PF<sub>6</sub>], is used as gelation solvent.[29, 38]

### 3.1. Morphology of gel phases



The morphology of the gel phases was observed with POM. For the hydrogels, SEM of the corresponding xerogels was also performed to further investigate the structure. In general, gels at 5 wt% of gelator concentration were analysed.

**Figure 1.** POM images of gels at 5 wt % of gelator: **a)** [C<sub>18</sub>mim][Br]/[bmim][PF<sub>6</sub>]; **b)** [C<sub>18</sub>mim][gluconate]/[bmim][PF<sub>6</sub>]; **c)** [C<sub>18</sub>mim]<sub>2</sub>[saccharate]/[bmim][PF<sub>6</sub>]; **d)** [C<sub>18</sub>mim][Br]/SW; SEM images of xerogel derived from **e-f)** [C<sub>18</sub>mim][Br]/SW; **g)** [C<sub>18</sub>mim][gluconate]/SW; **h-i)** [C<sub>18</sub>mim]<sub>2</sub>[saccharate]/SW.

Gels formed by [C<sub>18</sub>mim][Br] show a dense fibrous morphology both in IL and water (Figure 1a and 1d), where fibres of small dimensions can be observed. This highly ordered network is lost for

gels of **[C<sub>18</sub>mim][gluconate]**, which is characterized by a dense texture (Figure 1b) frequently observed for ionogels.[29, 38] On the other hand, ionogels formed by **[C<sub>18</sub>mim]<sub>2</sub>[saccharate]** also present a fibre like network (Figure 1c), but with fewer and longer fibres than that of the **[C<sub>18</sub>mim][Br]** ionogel.

POM investigation supports the previous hypothesis that the **[C<sub>18</sub>mim][Br]** and **[C<sub>18</sub>mim]<sub>2</sub>[saccharate]** gelators have a higher degree of structural order than **[C<sub>18</sub>mim][gluconate]**. Indeed, the higher  $T_{ge1}$  of gels derived from **[C<sub>18</sub>mim]<sub>2</sub>[saccharate]** is probably caused by the more organised self-assembled network.

SEM images of the xerogels reflect the same analysis (Figure 1e-i). In particular, for **[C<sub>18</sub>mim][Br]** in SW, the image (Figure 1e) shows several entangled fibres and, at higher magnification, a lamellar morphology can be observed (Figure 1f). On the other hand, the morphology of single objects seems partially hidden in the case of **[C<sub>18</sub>mim][gluconate]** in SW (Figure 1g) where only some round aggregates can be recognized (Figure S3d). Even for **[C<sub>18</sub>mim]<sub>2</sub>[saccharate]** in SW is difficult to define the morphology of the gel network (Figure 1h). However, in this case, a higher magnification view offers some evidence for a “chip” like geometry of gel aggregates (Figure 1i). Finally, **[C<sub>18</sub>mim]<sub>2</sub>[saccharate]** in PBS (1x) shows a round morphology (Figure S3e) with the presence of small fibres (Figure S3f).

This study indicates that the gel morphology is influenced by the gelation solvent. For example, all ionogels in **[bmim][NTf<sub>2</sub>]** present a dense texture (Figure S3a-c), where no single type of feature can be recognized.

### 3.2. Rheological properties

Rheological measurements confirmed the gel-like behaviour of the soft materials. In particular, stress and frequency sweeps were carried out. As shown in Figure 2a, for all gels the storage modulus ( $G'$ ) is higher than the loss modulus ( $G''$ ) at low stress, until both moduli reach the same value at the yield stress ( $\tau$ ). Beyond this point, an inversion of moduli occurs, and therefore, the yield stress indicates the value of stress that the gel needs to flow.[48] On the other hand, when measurements are performed within the linear viscoelastic region (LVR), both moduli are independent of the angular frequency (Figure 2b), and  $G'$  is always higher than  $G''$ . In addition, the stiffness of the gel,  $\tan \delta = G''/ G'$ , is always lower than 1, indicating the presence of strong colloidal forces (Table 3). The lower the ratio between the moduli, the higher the stiffness of the gel.

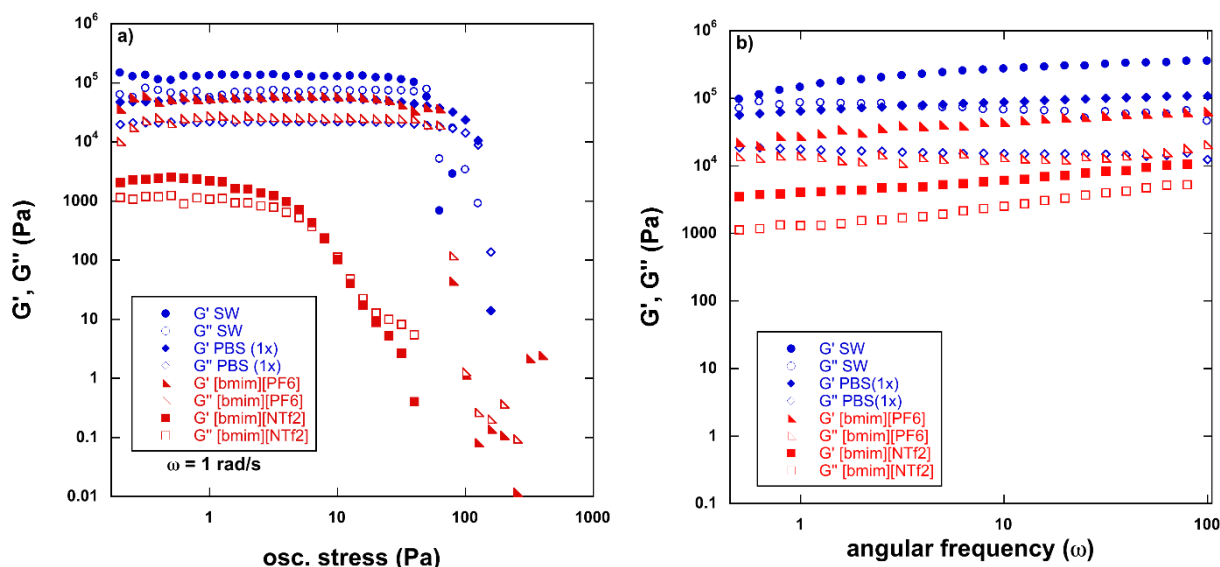


Figure 2. a) Stress and b) frequency sweeps of gels formed by  $[C_{18}mim]_2[saccharate]$ .

Table 3.  $G'$  and  $G''$ ,  $\tan \delta = G''/G'$  and values of  $\tau$  at  $G' = G''$  for gels investigated at 5 wt% gelator concentrations and 20 °C. Error limits are based on average of three different measurements with different aliquots of gels.

Gel	$G'$ (Pa)	$G''$ (Pa)	$\tan \delta$	$\tau$ $G'=G''$ (Pa)
$[C_{18}mim][Br]$ in $[bmim][PF_6]$	$32700 \pm 4700^b$	$4000 \pm 400^b$	$0.12 \pm 0.02^b$	$63 \pm 5$
$[C_{18}mim][Br]$ in $[bmim][NTf_2]$	$111000 \pm 25000^b$	$50000 \pm 10000^b$	$0.45 \pm 0.09^b$	$4 \pm 1$
$[C_{18}mim][Br]$ in PBS (1x)	$20890 \pm 680^a$	$6300 \pm 70^a$	$0.30 \pm 0.03^a$	$64 \pm 4$
$[C_{18}mim][Br]$ in SW	$175000 \pm 18000^b$	$40300 \pm 3400^b$	$0.23 \pm 0.05^b$	$125 \pm 9$
$[C_{18}mim][gluconate]$ in $[bmim][PF_6]$	$22400 \pm 300^a$	$2120 \pm 80^a$	$0.09 \pm 0.02^a$	$200 \pm 10$
$[C_{18}mim][gluconate]$ in $[bmim][NTf_2]$	$1250 \pm 90^b$	$440 \pm 40^b$	$0.35 \pm 0.06^b$	$13 \pm 4$
$[C_{18}mim][gluconate]$ in PBS (1x)	$2900 \pm 200^a$	$1120 \pm 70^a$	$0.38 \pm 0.04^a$	$125 \pm 8$
$[C_{18}mim][gluconate]$ in SW	$14100 \pm 3500^a$	$4800 \pm 100^a$	$0.34 \pm 0.06^a$	$200 \pm 8$
$[C_{18}mim]_2[saccharate]$ in $[bmim][PF_6]$	$30500 \pm 3400^a$	$14400 \pm 400^a$	$0.47 \pm 0.05^a$	$79 \pm 5$
$[C_{18}mim]_2[saccharate]$ in $[bmim][NTf_2]$	$3100 \pm 900^b$	$1180 \pm 120^b$	$0.37 \pm 0.03^b$	$8 \pm 1$
$[C_{18}mim]_2[saccharate]$ in PBS (1x)	$54000 \pm 10000^a$	$23200 \pm 5600^a$	$0.43 \pm 0.08^a$	$120 \pm 4$
$[C_{18}mim]_2[saccharate]$ in SW	$142000 \pm 4000^a$	$80000 \pm 5600^a$	$0.56 \pm 0.02^a$	$50 \pm 6$

<sup>a</sup> $G'$ ,  $G''$ ,  $\tan \delta$  at osc. stress = 3 Pa; <sup>b</sup> $G'$ ,  $G''$ ,  $\tan \delta$  at osc. stress = 1 Pa.

In general, the weakest gels are the ones formed in  $[bmim][NTf_2]$ , whilst all rheological parameters are almost comparable for the ionogels in  $[bmim][PF_6]$ , and all the hydrogels (Figure 2 and S4). Once again, these results reflect the thermal stability of the gels and can be ascribed to different interactions between the gelator and solvent molecules.

All the hydrogels, and the ionogels in  $[bmim][PF_6]$  exhibit high strength, an important property in the context of the potential environmental application of the gels since they are required to support the weight of the wastewater being treated. In particular, the magnitude of  $G'$  detected for these

supramolecular gels is higher than some polymeric gels,[49] and the yield stress in some cases is up to 200 Pa, an extremely high value for gels formed through supramolecular interactions.

Changing the gelator does not significantly influence the rheological properties of the gels. However, [C<sub>18</sub>mim][Br] gels exhibit a lower  $\tan \delta$  (Table 3) than the carbohydrate gels. The higher stiffness of the bromide gels reinforces the hypothesis of a strong association among the particles for these gels, deriving from the dense fibrous network (Figure 1e).

Rheological data do not suggest that these soft materials are responsive to external stimuli. Some of them (*i.e.* some hydrogels formed by [C<sub>18</sub>mim][Br] and [C<sub>18</sub>mim][gluconate]) are able to reform after disruption by using ultrasound irradiation, therefore showing sonotropic behaviour.[50] However, the vast majority are not sensitive to irradiation. Similarly, none of them exhibit thixotropic character, *i. e.* it is not possible to restore them after mechanical disruption (Table S3).

### 3.3. Kinetics of gel formation

The gel formation was studied by following the gel opacity (through its absorbance at 568 nm), which is qualitatively related to the number and size of polydisperse nanostructures in a system and, therefore, to the crystallinity of the gels.[51] For all hydrogels, and the ionogels in [bmim][PF<sub>6</sub>], a one-step formation mechanism is observed (Figure 3 and S5). In some cases, a short induction time is followed by gel formation and equilibration (Table S4).

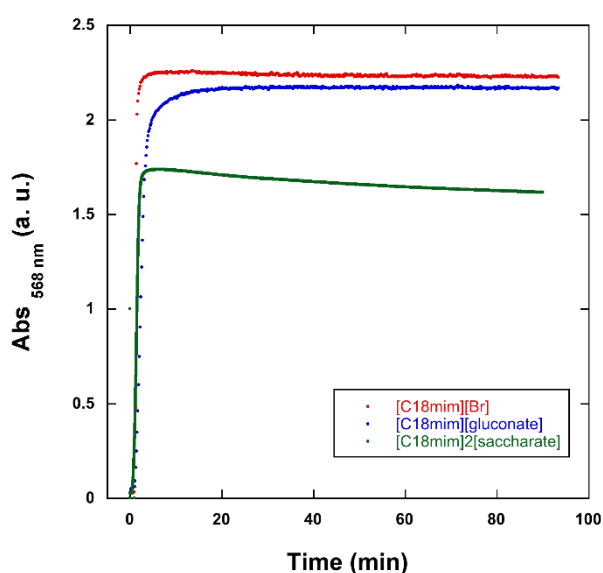


**Figure 3.** Kinetics of gel formation for gels in SW at 5 wt %, measurements recorded at 568 nm through UV-vis spectroscopy.

For the ionogels in [bmim][NTf<sub>2</sub>], a two-step formation mechanism is observed (Figure S5). The absorbance increases reaching a constant value for almost 20 min in a first step, then it further increases until the formation of a plateau region corresponding to the completion of gelation. This behaviour has been previously attributed to initial formation of fibers (*i.e.*, 1D objects) before the 3D networks of self-assembled fibrillar networks are completed.[30, 38] In addition, gel formation is much slower than in the other cases, and for [C<sub>18</sub>mim][Br] in [bmim][NTf<sub>2</sub>], it is even too slow to be recorded under the experimental conditions used. The mechanism of gel formation, combined with its morphology, indicates that the interactions connecting gelator and solvent particles for gels in [bmim][NTf<sub>2</sub>] are weak, whereas a strong association can be hypothesized for hydrogels and gels in [bmim][PF<sub>6</sub>].

For gels in SW and [bmim][PF<sub>6</sub>], in two out of three cases, the gelation times are comparable (Table S4), whilst the opacity, and hence crystallinity of the gels is lower for the saccharate analogues. This is probably due to the formation of smaller aggregates within the self-assembled network that has been observed in the saccharate derived gels (Figure 1c and 1i). A different scenario is observed in PBS (1x), where the gluconate derived gel formation is slower than that of the other gelators. Hence, structural differences in the gelators are reflected in the gelation times, when a gelation solvent with a lower ionic strength is used. Gels of [C<sub>18</sub>mim][Br], with the only exception of [bmim][NTf<sub>2</sub>], which exhibits a fast formation time, and almost the same opacity value independent of the gelation solvent (Table S4 and Figure S5).

### 3.4. Cr(VI) adsorption of gels

The ability of these gels to adsorb water solutions of Cr(VI) was tested in static conditions, by layering wastewater onto the gel surface (Figure 4a). The adsorption process is visible, as the yellow solution turns colourless and gel surface turns yellow after a certain time of contact (Figure 4b). Interestingly in some cases, after a prolonged exposure to Cr(VI) solution, the gel surface turned green (Figure 4c), suggesting the reduction of Cr(VI) to Cr(III), *vide infra* (Cr(VI) reduction).

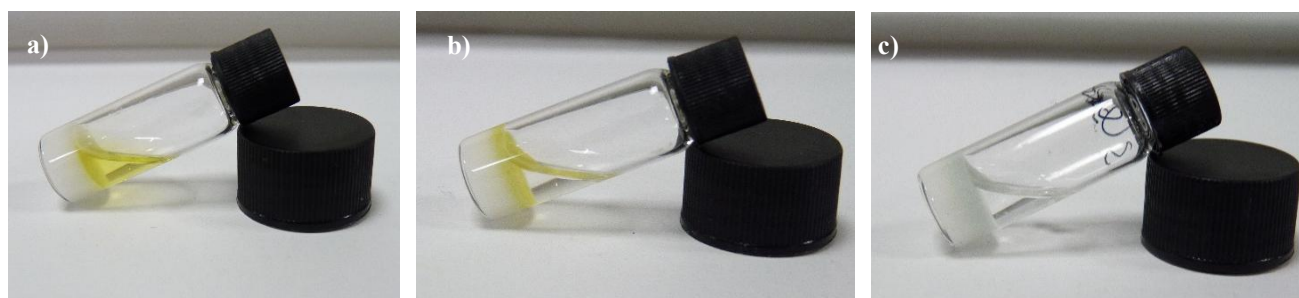


**Figure 4.** Cr(VI) water solution ( $1.7 \cdot 10^{-3}$  M) in contact with hydrogel –  $[\text{C}_{18}\text{mim}]_2[\text{saccharate}]$  in SW – **a)** immediately after the casting of the solution; **b)** after 24 h, gel surface turns yellow and water solution uncoloured; **c)** after 48 h, gel surface turns green.

The removal efficiency (RE) of Cr(VI) from aqueous solution was spectrophotometrically determined, by monitoring the decreasing intensity of the Cr(VI) UV band, with a maximum absorption at 350 nm (Figure S6). The gels resisted the weight of the water in agreement with good rheological strength, and  $^1\text{H}$  NMR analysis verified that there was effectively no release of any component from the gel into the water solution (Figure S7 and Table S6). This confirms the “greenness” of the entire process, a key factor for the environmental application of supramolecular gels.[17]

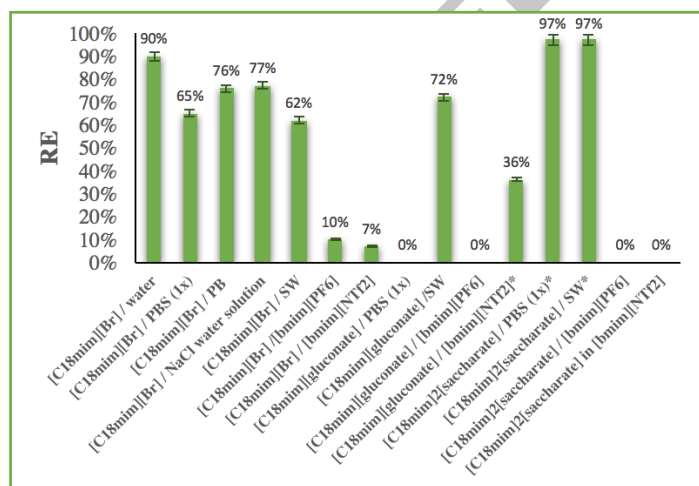


**Figure 5.** RE of gels adsorption of Cr(VI) ( $1.7 \cdot 10^{-3}$  M) after 24h of contact. \*after 48 h the gel surface turns dark green instead of yellow. RE based on duplicate with reproducibility of 2%.

In Figure 5, the RE's for all gels, after the same exposure time are compared. In general, all hydrogels display a better adsorption efficiency than the corresponding ionogels, which are destroyed after contact with the solution ( $[\text{C}_{18}\text{mim}][\text{gluconate}]/[\text{bmim}][\text{PF}_6]$ ), or do not completely adsorb the metal solution as in the case of saccharate-ionogels. This behaviour is in contrast with

the good removal efficiency that some similar ionogels used for dye adsorption,[31] and can be ascribed to the higher affinity of Cr(VI) for the aqueous environment than the IL. Indeed, a clear relationship between gel properties and the adsorption behaviour cannot be determined as function of gelation solvent. On one hand, [bmim][NTf<sub>2</sub>] ionogels are the weakest gels in term of  $T_{gel}$  and rheological properties, on the other hand [bmim][PF<sub>6</sub>] ionogels showed comparable properties to hydrogels.

However, comparison of the hydrogels demonstrates that the carbohydrate-derived gels have better adsorption capacities compared to the bromide hydrogel, as 97% and 72% RE, instead of 62% have been achieved respectively in [C<sub>18</sub>mim]<sub>2</sub>[saccharate]/SW, [C<sub>18</sub>mim][gluconate]/SW and [C<sub>18</sub>mim][Br] /SW. In addition, 97% RE has been also reached in [C<sub>18</sub>mim]<sub>2</sub>[saccharate]/PBS (1x) compared to 77% of [C<sub>18</sub>mim][Br] /PBS (1x). Unfortunately the [C<sub>18</sub>mim][gluconate]/PBS (1x) hydrogel did not resist prolonged contact with the water solution. To further investigate the influence of the gelator in the adsorption process, adsorption kinetics were measured in batch experiments on gels in SW (Figure 6).

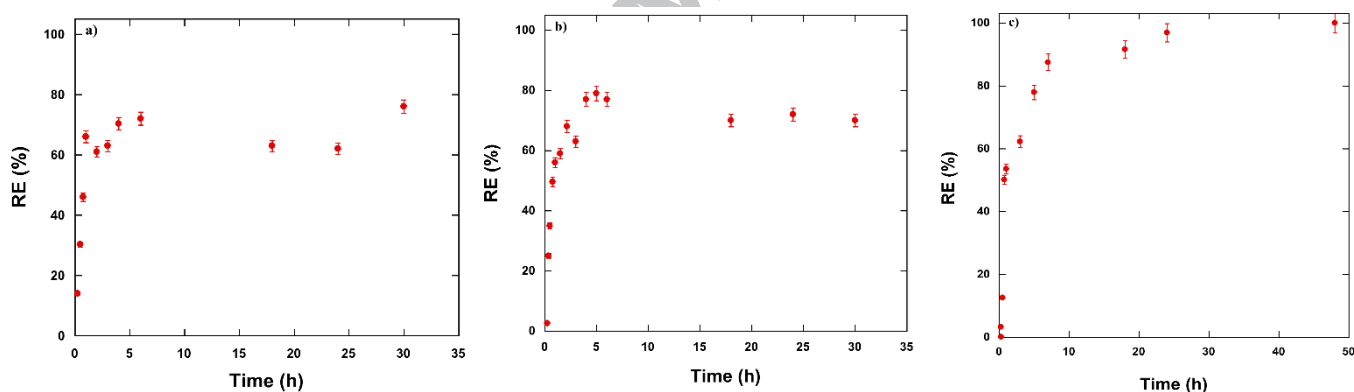


**Figure 6.** Kinetics of Cr(VI) ( $1.7 \cdot 10^{-3}$  M) adsorption for gels in SW of a) [C<sub>18</sub>mim][Br], b) [C<sub>18</sub>mim][gluconate] and c) [C<sub>18</sub>mim]<sub>2</sub>[saccharate]. RE based on duplicate experiments with reproducibility of 2%.

All gels initially have fast adsorption kinetics, reaching 60 % removal efficiency in almost 3 h and 1.5 h for the [C<sub>18</sub>mim][gluconate] hydrogel. This behavior has been previously observed, and attributed to the concentration gradient at higher initial metal concentrations, which drives the transfer of metal ions from the bulk solution to the surface of the adsorbent.[52] Even in the adsorption process of some chitosan polymers, equilibrium was achieved after almost 24 h, following an initially fast adsorption.[53] It is likely that, at the beginning, the higher availability of adsorption sites enhances the adsorption process, but when the adsorbent surface became progressively covered by metal ions, the number of available adsorption sites decreases and sites are deeper within the gel and therefore the adsorption rate is slower.[54] In addition, after prolonged

exposure to Cr(VI) solutions hydrogels of  $[\text{C}_{18}\text{mim}][\text{Br}]$  and  $[\text{C}_{18}\text{mim}][\text{gluconate}]$  showed a slight decrease in RE that is probably due to the presence of an equilibrium established between the Cr(VI) adsorbed on the gel phase and ions partially released back in water solution. However, the  $[\text{C}_{18}\text{mim}]_2[\text{saccharate}]$  hydrogel did not show this trend, as RE increased continuously and stayed constant after reaching equilibrium.

The  $[\text{C}_{18}\text{mim}]_2[\text{saccharate}]$  hydrogel seems to be the best adsorption system, achieving total removal efficiency after 24 h. This gel exhibits the lowest stiffness and so, probably, when weaker colloidal forces are active, the gel matrix is more available to accept metal ions. This hypothesis is consistent with the decrease in RE for SW gels as follows:  $[\text{C}_{18}\text{mim}]_2[\text{saccharate}] > [\text{C}_{18}\text{mim}][\text{gluconate}] > [\text{C}_{18}\text{mim}][\text{Br}]$  and this order corresponds to the simultaneously decreasing  $\tan \delta$  values, indicating higher stiffness of gels.

In addition, by testing the ability of individual gel components to adsorb Cr(VI) (Table S6), it is clear that there is a major contribution from the gel state, which is responsible for the adsorption process. Indeed, whilst the carbohydrate-derived gelators present some adsorption ability by themselves, this does not occur in the case of  $[\text{C}_{18}\text{mim}][\text{Br}]$ , which forms gels with lower adsorption capabilities. Nevertheless, the RE's of these gelators are much lower than the ones obtained for the hydrogel phases. So, a combined action between the gelator structure, and physical gel properties affects Cr(VI) removal ability.

In order to compare the adsorption capacity of the hydrogel with one of the few gels reported in the literature,  $q_e$ , the adsorption capacity at equilibrium (mg/g), was determined in a batch experiment where a small amount of gel was immersed in a large volume of Cr(VI) solution (Figure S8). The adsorption capacities obtained are extremely high, with  $q_e$  values of 272 and 598 mg/g obtained from experiments with 10 mL and 20 mL of Cr(VI) solution, respectively. These results are a significant improvement on other gel systems or adsorbents reported in the literature for use as Cr(VI) adsorbents (Table 4).

Furthermore, it is well known that the best adsorption capacity is obtained at low pH values, thanks to the mechanism of Cr(VI) interaction with sorbents.[55] However, working at a neutral pH allows minimal alteration to the natural environment of the contaminated water system.

**Table 4.** Adsorption capacity of different systems.

Adsorbents system for Cr(VI) removal	Time (h)	pH	q <sub>e</sub> (mg/g)
Carbohydrate-derived hydrogel (this work)	24	7.4	598
Sponge-like Chitosan/Reduced Graphene Oxide/Montmorillonite Composite Hydrogels[15]	3	2.0	64
3D folic acid polyaniline hybrid hydrogel[16]	4	7.0	153
2-mercaptobenzimidazole copper(II) chloride metallogel[14]	10	7.5	81
agarose-Fe nanoparticles hydrogel[56]	24	5.8	19
Nanocomposite polymeric film of chitosan, carbon nanofibers and Fe nanoparticles[57]	1.3	5.2	80
Molybdenum disulfide coated Mg/Al layered double hydroxide composites[58]	24	5.0	76

### 3.5. Cr(VI) reduction

The chemisorption process for Cr(VI) removal has also been observed for some polyaniline hydrogels and it has been ascribed to oxidation of the aryl amine –NH sites of the polymer into imine groups.[16, 59] However, those studies were carried out under acidic pH conditions, so in our case, it is likely that another functionality is responsible for the reduction process. Remembering the high potential of aldaric acid to form complexes with metal species,[39, 60-62] we tested the ability of saccharic acid potassium salt to reduce Cr(VI) as a model of what could occur on our carbohydrate-based gels after Cr (VI) adsorption causes the colour to change (Figure 4c).

In particular, a green powder was isolated from the reaction mixture (see SI) and a colour change from yellow to green was also observed when the same reaction was carried out in D<sub>2</sub>O solution in an NMR tube (Figure S9). Figure 7 shows <sup>1</sup>H NMR spectra of saccharic acid potassium salt in D<sub>2</sub>O and of the reaction mixture with chromate at different time intervals. The progressive reduction of Cr(VI) to Cr(III) is evident from the disappearance of saccharate protons and from the gradual broadening of all peaks due to the formation of the paramagnetic Cr(III) species.

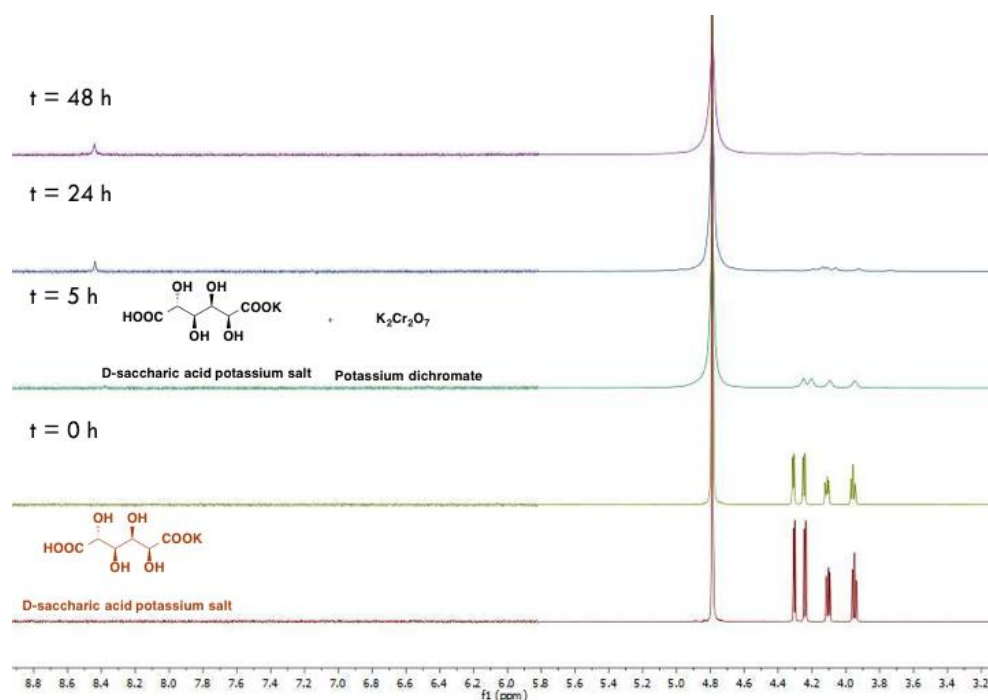


**Figure 7.** <sup>1</sup>H NMR spectra of D-saccharic acid potassium salt in D<sub>2</sub>O (red) and the reaction mixture of D-saccharic acid potassium salt and potassium dichromate in D<sub>2</sub>O at different intervals of time.

To correlate this analysis with what occurs on the gels, we carried out IR and SEM analysis on the xerogels, 48 h after the adsorption of Cr(VI). After a prolonged exposure time (> 72 h) of the gel to the Cr(VI) solution, the entire gel turned green (Figure S10), so the chemisorption process involves and influences the entire gel matrix and not only the surface of the gel. The superposition of IR spectra of the pure xerogel, and the xerogel after 24 h and 48 h of Cr(VI) adsorption shows the appearance of new bands corresponding to the presence of a Cr(III) species. In particular, for the green coloured xerogel after 48 h (green line in Figure S11a), bands at 1337 cm<sup>-1</sup> and 1618 cm<sup>-1</sup> are visible. These bands are missing in the pure and 24 h exposed xerogel, indicating the initial physical adsorption of Cr(VI), whilst they are similar to the bands at 1362 cm<sup>-1</sup> and 1607 cm<sup>-1</sup> present in the green complex isolated from the reaction performed in the presence of saccharic acid potassium salt (blue line in Figure S11b). Finally, SEM analysis on the xerogel after 48 h of exposure to Cr(VI) reveals a completely changed morphology with respect to the pure xerogel (see Figure 1h-i and 8).

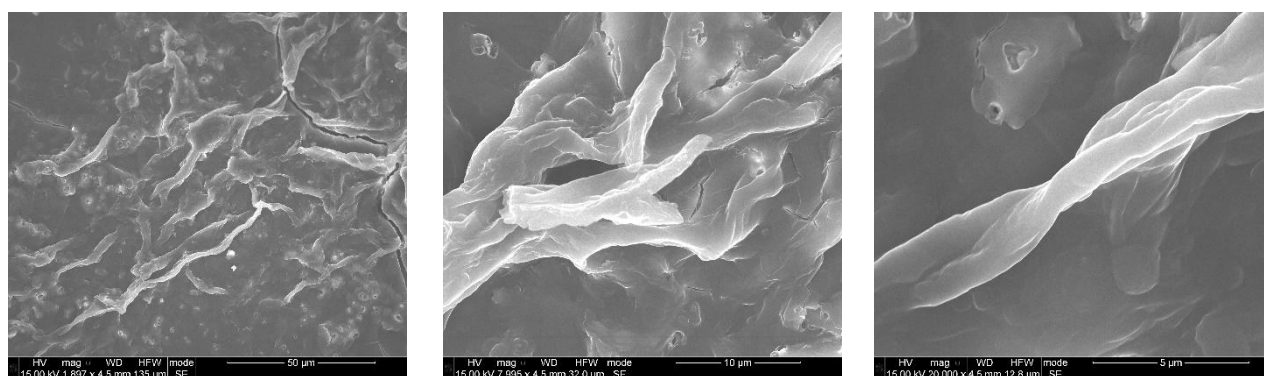


**Figure 8.** SEM images of xerogel derived from  $[\text{C}_{18}\text{mim}]_2[\text{saccharate}]/\text{SW}$  after 48 h of gel exposure to Cr(VI) solution, at different magnifications.

The processes of adsorption and reduction of Cr(VI) clearly influenced gel features, as shown from the fibrillar morphology recognizable after 48h of exposure of the gel to Cr(VI) solution (Figure 8). This dense fibrous network is completely different from the “chip” like geometry of gel aggregates (Figure 1i) observed before the chromium reduction. This process represents a procedure to adsorb a toxic metal and to convert it into a less toxic species. This is a process of chemisorption and it is well in line with previous report in literature about the ability of sugar acids, in particular saccharic acid, to reduce Cr(VI) species.[63] This process can be extremely convenient considering that, with only one material, two purification steps are obtained at the same time. For example, electrochemical heavy metal wastewater treatment techniques have been successfully applied for the reduction of Cr(VI) to Cr(III) because they warrant a fast and well-controlled process, providing good reduction yields.[64] However, the high initial capital investment and the expensive electricity supply needed for the realization of electrochemical technologies limits its development.[5] So, in this approach, the combination of the adsorption/reduction process exerted by a simple hydrogel could minimize operational costs. In addition, the adsorption is efficient even at low concentration of metal.

Furthermore, remembering that after a contact time of 24 h, the hydrogel preserves its gel consistency, we examined the reuse of this sorbent system to decrease the impact of the remediation intervention on the environment.[40] In particular, after the first adsorption of chromium water solution, the best sorbent gel, *i.e.*  $[\text{C}_{18}\text{mim}]_2[\text{saccharate}]$  in SW, was put in contact with a fresh chromium aqueous sample and, proved able to adsorb the metal for 4 cycles with a gradual loss of efficiency after the third cycle (Figure 9).

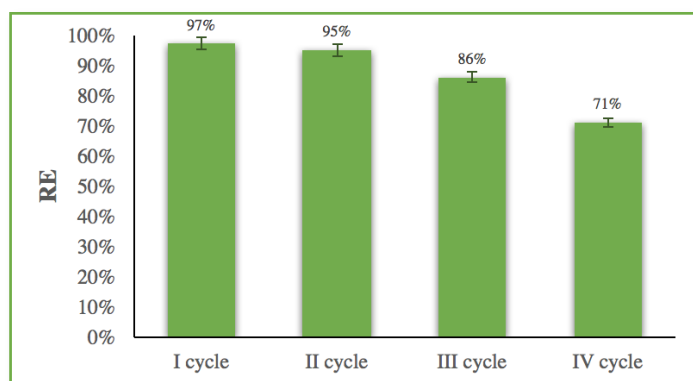


**Figure 9.** Cycles of reusing of  $[\text{C}_{18}\text{mim}]_2[\text{saccharate}]$  in SW at 5 wt % in the adsorption of Cr(VI) ( $1.7 \cdot 10^{-3} \text{ M}$ ) at  $25 \text{ }^\circ\text{C}$  and after 24 h. RE based on duplicate with reproducibility of 2%.

### 3.6. Adsorption of other metals

Considering the good performance of these gels in the adsorption of Cr(VI), the adsorption of divalent metals was also tested. Solutions of divalent metals, such as copper(II) nitrate hemi(pentahydrate), cobalt(II) nitrate hexahydrate, zinc(II) nitrate monohydrate and nickel(II) nitrate hexahydrate, were layered for 24 h on  $[\text{C}_{18}\text{mim}]_2[\text{saccharate}]/\text{SW}$ ; used in this case as a model gel. However, due to the low molar extinction coefficient of the metals, Alizarin Red S was necessary to spectrophotometrically detect the species in solution.[44] Alizarin Red S, when coordinated with tetraborate, forms an orange solution that turns pink/red in colour, in the presence of divalent metals (Figure S12). This colour change reflects in the bathochromic shift of the Alizarin Red S bands (Figure S13).

The gel of  $[\text{C}_{18}\text{mim}]_2[\text{saccharate}]/\text{SW}$  was not able to adsorb any of the four divalent metal solutions tested, evidenced by the fact that the absorption band of the complex did not show any decrease in intensity after 24 h of contact with gel phase (Figure S13). Hence, the gel is selective for the adsorption of Cr(VI) solutions. A similar behaviour has been previously observed for some polymeric xerogels, which are able to remove the oxyanionic pollutant  $\text{Cr}_2\text{O}_7^{2-}$ , but not cationic ones such as  $\text{Hg}^{2+}$  and  $\text{Pb}^{2+}$ . [16] This selectivity has been ascribed to the electrostatic interactions between the oppositely charged adsorbent and adsorbate. However, for the hydrogels in this work, other factors can cooperate in the adsorption process, because the gelator comprises both cationic and anionic components and the anion features multiple hydrogen bonding groups. In general, the selectivity of uptake is an important property in the water treatment especially for some specific industrial settings where it may be beneficial to select and optimise the removal capacity of the sorbent for a particular metal.[17]

#### 4. Conclusions

In conclusion, supramolecular gels can be used for wastewater treatment and behave as efficient sorbents for Cr(VI) removal. In particular, the adsorption efficiency can be tuned through gel properties that vary as function of the nature of the gelator anion and gelation solvent.

Only the supramolecular hydrogels are able to selectively adsorb Cr(VI) from water solutions at a neutral *pH*. Amongst the hydrogels, the carbohydrate derived systems show the best adsorption performance (RE of 97% in 24h). This is ascribable to the lower stiffness of the gel that results in a higher adsorbing capacity due to less strong colloidal forces within the gel network, that do not compete with the adsorption process. The most efficient gel reaches an adsorbing capacity of 598 mg/g which is a significant improvement on other gel systems for which a maximum value of 153 mg/g has been reported.[14, 16, 58] In addition, the gel can be recycled up to 4 times.

Interestingly, gels formed by the gelator with saccharate dianion show chemisorption that allows conversion of the metal into a less toxic species. This process can be extremely convenient considering that, with only one material, two steps of purification can be obtained at the same time.

In this approach, the combination of the adsorption/reduction process exerted by a simple hydrogel should minimize the operational costs of water treatment. On the other hand, the attempt to use the present hydrogels in the removal of different cationic metal species clearly demonstrates how in the sorption mechanism the sugar based anion exerts a dual role. Firstly, it acts as a coordinating ligand able to catch the oxyanionic pollutants, possibly through hydrogen bonding. Subsequently, it behaves as a reducing agent able to transform toxic Cr(VI) into Cr(III).

The gels here reported are mainly formed from water, and they are able to act at neutral *pH* without the addition of any metals or additives such as carbon nanomaterials. These gels retain their nature even after chromium adsorption without any leaching of the gelator, displaying excellent performance, selectivity and recycling ability. These positive results open the use of these tunable supramolecular gels for a wide range of applications, particularly wastewater treatment.

#### ASSOCIATED CONTENT

**Supporting Information.** The following files are available free of charge as PDF file. Supporting Information contains the DSC traces of gelators and gels, POM and SEM images, rheological graphs, kinetic of gel formation, UV spectra of Cr(VI) adsorption and calibration curve,  $^1\text{H}$  NMR spectra for the gelator release in water, IR spectra after Cr(VI) adsorption and reduction, UV spectra

for other metal adsorption, gelation and  $T_{gel}$  tables, tables reporting removal efficiency for the different systems studied.

#### ACKNOWLEDGMENT

We thank MIUR (FIRB 2010RBF10BF5V) and University of Palermo (FFR 2018) for financial support. CR thanks Project PERFEST 2017 granted by Università degli Studi di Palermo and Durham University for hospitality received.

#### REFERENCES

- [1] R.K. Sharma, A. Adholeya, M. Das, A. Puri, CHAPTER 2 Green Materials for Sustainable Remediation of Metals in Water, Green Materials for Sustainable Water Remediation and Treatment, The Royal Society of Chemistry 2013, pp. 11-29.
- [2] V. Vetriselvi, R. Jaya Santhi, Redox polymer as an adsorbent for the removal of chromium (VI) and lead (II) from the tannery effluents, Water Resources and Industry, 10 (2015) 39-52.
- [3] T. Chen, Z. Zhou, S. Xu, H. Wang, W. Lu, Adsorption behavior comparison of trivalent and hexavalent chromium on biochar derived from municipal sludge, Bioresour. Technol., 190 (2015) 388-394.
- [4] K. Grace Pavithra, P. Senthil Kumar, F. Carolin Christopher, A. Saravanan, Removal of toxic Cr(VI) ions from tannery industrial wastewater using a newly designed three-phase three-dimensional electrode reactor, J. Phys. Chem. Solids, 110 (2017) 379-385.
- [5] F. Fu, Q. Wang, Removal of heavy metal ions from wastewaters: A review, J. Environ. Manage., 92 (2011) 407-418.
- [6] D. Mohan, K.P. Singh, V.K. Singh, Removal of Hexavalent Chromium from Aqueous Solution Using Low-Cost Activated Carbons Derived from Agricultural Waste Materials and Activated Carbon Fabric Cloth, Ind. Eng. Chem. Res., 44 (2005) 1027-1042.
- [7] X. Zhang, Y. Lei, Y. Yuan, J. Gao, Y. Jiang, Z. Xu, S. Zhao, Enhanced removal performance of Cr(VI) by the core-shell zeolites/layered double hydroxides (LDHs) synthesized from different metal compounds in constructed rapid infiltration systems, Environ. Sci. Pollut. R., 25 (2018) 9759-9770.
- [8] M. Mobarak, A.Q. Selim, E.A. Mohamed, M.K. Seliem, A superior adsorbent of CTAB/H2O2 solution-modified organic carbon rich-clay for hexavalent chromium and methyl orange uptake from solutions, J. Mol. Liq., 259 (2018) 384-397.
- [9] X. Wang, R. Peng, H. He, X. Yan, S. Zhu, H. Zhao, D. Deng, Y. Qiongwei, Y. Lei, L. Luo, Nanomagnetic polyhedral oligomeric silsesquioxanes composite derived sulfur-containing adsorbents for effective elimination of hexavalent chromium and organic cationic dyes from water, Colloids Surf., A, 550 (2018) 1-8.
- [10] W. Lu, J. Li, Y. Sheng, X. Zhang, J. You, L. Chen, One-pot synthesis of magnetic iron oxide nanoparticle-multiwalled carbon nanotube composites for enhanced removal of Cr(VI) from aqueous solution, J. Colloid Interface Sci., 505 (2017) 1134-1146.
- [11] M. Kazemi, M. Jahanshahi, M. Peyravi, Hexavalent chromium removal by multilayer membrane assisted by photocatalytic couple nanoparticle from both permeate and retentate, J. Hazard. Mater., 344 (2018) 12-22.
- [12] S. Periyasamy, V. Gopalakannan, N. Viswanathan, Fabrication of magnetic particles imprinted cellulose based biocomposites for chromium(VI) removal, Carbohydr. Polym., 174 (2017) 352-359.

- [13] M.K. Dinker, P.S. Kulkarni, Recent Advances in Silica-Based Materials for the Removal of Hexavalent Chromium: A Review, *J. Chem. Eng. Data*, 60 (2015) 2521-2540.
- [14] S. Sarkar, S. Dutta, P. Bairi, T. Pal, Redox-Responsive Copper(I) Metallogel: A Metal-Organic Hybrid Sorbent for Reductive Removal of Chromium(VI) from Aqueous Solution, *Langmuir*, 30 (2014) 7833-7841.
- [15] P. Yu, H.-Q. Wang, R.-Y. Bao, Z. Liu, W. Yang, B.-H. Xie, M.-B. Yang, Self-Assembled Sponge-like Chitosan/Reduced Graphene Oxide/Montmorillonite Composite Hydrogels without Cross-Linking of Chitosan for Effective Cr(VI) Sorption, *ACS Sustainable Chem. Eng.*, 5 (2017) 1557-1566.
- [16] S. Das, P. Chakraborty, R. Ghosh, S. Paul, S. Mondal, A. Panja, A.K. Nandi, Folic Acid-Polyaniline Hybrid Hydrogel for Adsorption/Reduction of Chromium(VI) and Selective Adsorption of Anionic Dye from Water, *ACS Sustainable Chem. Eng.*, 5 (2017) 9325-9337.
- [17] B.O. Okesola, D.K. Smith, Applying low-molecular weight supramolecular gelators in an environmental setting - self-assembled gels as smart materials for pollutant removal, *Chem. Soc. Rev.*, 45 (2016) 4226-4251.
- [18] H. Guo, T. Jiao, Q. Zhang, W. Guo, Q. Peng, X. Yan, Preparation of Graphene Oxide-Based Hydrogels as Efficient Dye Adsorbents for Wastewater Treatment, *Nanoscale Res. Lett.*, 10 (2015) 272.
- [19] N.M. Sangeetha, U. Maitra, Supramolecular gels: Functions and uses, *Chem. Soc. Rev.*, 34 (2005) 821-836.
- [20] J.W. Steed, Supramolecular gel chemistry: developments over the last decade, *Chem. Commun.*, 47 (2011) 1379-1383.
- [21] P. Terech, R.G. Weiss, Low Molecular Mass Gelators of Organic Liquids and the Properties of Their Gels, *Chem. Rev. (Washington, DC, U. S.)*, 97 (1997) 3133-3160.
- [22] C.D. Jones, J.W. Steed, Gels with sense: supramolecular materials that respond to heat, light and sound, *Chem. Soc. Rev.*, 45 (2016) 6546-6596.
- [23] P. Wasserscheid and T. Welton, *Ionic Liquids in Synthesis*, 2nd ed., Wiley-VCH, Weinheim, Germany, 2008.
- [24] R.D. Rogers, K.R. Seddon, Ionic Liquids--Solvents of the Future?, *Science*, 302 (2003) 792.
- [25] M. Freemantle, *An Introduction to Ionic Liquids*, RSC Publications, Cambridge, UK, 2010.
- [26] J. Le Bideau, L. Viau, A. Vioux, Ionogels, ionic liquid based hybrid materials, *Chem. Soc. Rev.*, 40 (2011) 907-925.
- [27] P.C. Marr, A.C. Marr, Ionic liquid gel materials: applications in green and sustainable chemistry, *Green Chem.*, 18 (2016) 105-128.
- [28] Y. Ding, J. Zhang, L. Chang, X. Zhang, H. Liu, L. Jiang, Preparation of High-Performance Ionogels with Excellent Transparency, Good Mechanical Strength, and High Conductivity, *Adv. Mater.*, 29 (2017) 1704253.
- [29] C. Rizzo, R. Arrigo, T. Dintcheva Nadka, G. Gallo, F. Giannici, R. Noto, A. Sutura, P. Vitale, F. D'Anna, Supramolecular Hydro- and Ionogels: A Study of Their Properties and Antibacterial Activity, *Chem. Eur. J.*, 23 (2017) 16297-16311.
- [30] C. Rizzo, F. Arcudi, L. Đorđević, N.T. Dintcheva, R. Noto, F. D'Anna, M. Prato, Nitrogen-Doped Carbon Nanodots-Ionogels: Preparation, Characterization, and Radical Scavenging Activity, *ACS Nano*, 12 (2018) 1296-1305.
- [31] S. Marullo, C. Rizzo, N.T. Dintcheva, F. Giannici, F. D'Anna, Ionic liquids gels: Soft materials for environmental remediation, *J. Colloid Interface Sci.*, 517 (2018) 182-193.
- [32] K. Pohako-Esko, M. Bahlmann, P.S. Schulz, P. Wasserscheid, Chitosan Containing Supported Ionic Liquid Phase Materials for CO<sub>2</sub> Absorption, *Ind. Eng. Chem. Res.*, 55 (2016) 7052-7059.
- [33] F. Billeci, F. D'Anna, H.Q.N. Gunaratne, N.V. Plechkova, K.R. Seddon, "Sweet" Ionic Liquid Gels: Materials for Sweetening of Fuels, *Green Chem.*, (2018).

- [34] P.-F. Vittoz, H. El Siblani, A. Bruma, B. Rigaud, X. Sauvage, C. Fernandez, A. Vicente, N. Barrier, S. Malo, J. Levillain, A.-C. Gaumont, I. Dez, Insight in the Alginate Pd-Ionogels—Application to the Tsuji–Trost Reaction, *ACS Sustainable Chem. Eng.*, 6 (2018) 5192-5197.
- [35] F. D'Anna, R. Noto, Di- and Tricationic Organic Salts: An Overview of Their Properties and Applications, *Eur. J. Org. Chem.*, 2014 (2014) 4201-4223.
- [36] G. John, B. Vijai Shankar, S.R. Jadhav, P.K. Vemula, Biorefinery: A Design Tool for Molecular Gelators, *Langmuir*, 26 (2010) 17843-17851.
- [37] S. Datta, S. Bhattacharya, Multifarious facets of sugar-derived molecular gels: molecular features, mechanisms of self-assembly and emerging applications, *Chem. Soc. Rev.*, 44 (2015) 5596-5637.
- [38] C. Rizzo, F. D'Anna, R. Noto, M. Zhang, R.G. Weiss, Insights into the Formation and Structures of Molecular Gels by Diimidazolium Salt Gelators in Ionic Liquids or “Normal” Solvents, *Chem. Eur. J.*, 22 (2016) 11269-11282.
- [39] J. Dong, B. Liu, B. Yang, Synthesis, crystal structure and magnetic properties of trinuclear chromium(III) basic carboxylate assembly:  $[\text{Cr}_3\text{O}(\text{salH})_7(\text{H}_2\text{O})_2]$  (salH<sub>2</sub>=salicylic acid), a new member of  $[\text{Cr}_3\text{O}]$  family, *J. Mol. Struct.*, 1116 (2016) 311-316.
- [40] C. Rizzo, S. Marullo, P.R. Campodonico, I. Pibiri, N.T. Dintcheva, R. Noto, D. Millan, F. D'Anna, Self-Sustaining Supramolecular Ionic Liquid Gels for Dye Adsorption, *ACS Sustainable Chem. Eng.*, 6 (2018) 12453-12462.
- [41] S. Raghavan, B. Cipriano, *Gel Formation: Phase Diagrams Using Tabletop Rheology and Calorimetry* Springer, Dordrecht, 2006.
- [42] D.J. Abdallah, R.G. Weiss, n-Alkanes Gel n-Alkanes (and Many Other Organic Liquids), *Langmuir*, 16 (2000) 352-355.
- [43] O. Okesola Babatunde, K. Suravaram Sindhu, A. Parkin, K. Smith David, Selective Extraction and In Situ Reduction of Precious Metal Salts from Model Waste To Generate Hybrid Gels with Embedded Electrocatalytic Nanoparticles, *Angew. Chem., Int. Ed.*, 55 (2015) 183-187.
- [44] T. Yokoyama, K. Tashiro, T. Murao, A. Yanase, J. Nishimoto, M. Zenki, Determination of complex formation constants for Cu(II)–Alizarin complexone with amines by capillary zone electrophoresis, *Anal. Chim. Acta*, 398 (1999) 75-82.
- [45] R. Jadhav Swapnil, K. Vemula Praveen, R. Kumar, R. Raghavan Srinivasa, G. John, Sugar-Derived Phase-Selective Molecular Gelators as Model Solidifiers for Oil Spills, *Angew. Chem., Int. Ed.*, 49 (2010) 7695-7698.
- [46] V.A. Mallia, D.L. Blair, R.G. Weiss, Oscillatory Rheology and Surface Water Wave Effects on Crude Oil and Corn Oil Gels with (R)-12-Hydroxystearic Acid as Gelator, *Ind. Eng. Chem. Res.*, 55 (2016) 954-960.
- [47] M. Vibhute Amol, V. Muvvala, M. Sureshan Kana, A Sugar-Based Gelator for Marine Oil-Spill Recovery, *Angew. Chem., Int. Ed.*, 55 (2016) 7782-7785.
- [48] K. Almdal, J. Dyre, S. Hvidt, O. Kramer, Towards a phenomenological definition of the term ‘gel’, *Polymer Gels and Networks*, 1 (1993) 5-17.
- [49] A.L.B. Ramirez, Z.S. Kean, J.A. Orlicki, M. Champhekar, S.M. Elsagr, W.E. Krause, S.L. Craig, Mechanochemical strengthening of a synthetic polymer in response to typically destructive shear forces, *Nature Chem.*, 5 (2013) 757.
- [50] G. Cravotto, P. Cintas, Molecular self-assembly and patterning induced by sound waves. The case of gelation, *Chem. Soc. Rev.*, 38 (2009) 2684-2697.
- [51] P. Terech, D. Pasquier, V. Bordas, C. Rossat, Rheological Properties and Structural Correlations in Molecular Organogels, *Langmuir*, 16 (2000) 4485-4494.
- [52] X. Liu, L. Zhang, Insight into the adsorption mechanisms of vanadium(V) on a high-efficiency biosorbent (Ti-doped chitosan bead), *Int. J. Biol. Macromol.*, 79 (2015) 110-117.

- [53] M. Vakili, S. Deng, T. Li, W. Wang, W. Wang, G. Yu, Novel crosslinked chitosan for enhanced adsorption of hexavalent chromium in acidic solution, *Chem. Eng. J.*, 347 (2018) 782-790.
- [54] M. Vakili, M. Rafatullah, B. Salamatinia, M.H. Ibrahim, A.Z. Abdullah, Elimination of reactive blue 4 from aqueous solutions using 3-aminopropyl triethoxysilane modified chitosan beads, *Carbohydr. Polym.*, 132 (2015) 89-96.
- [55] B. Saha, C. Orvig, Biosorbents for hexavalent chromium elimination from industrial and municipal effluents, *Coord. Chem. Rev.*, 254 (2010) 2959-2972.
- [56] F. Luo, Z. Chen, M. Megharaj, R. Naidu, Simultaneous removal of trichloroethylene and hexavalent chromium by green synthesized agarose-Fe nanoparticles hydrogel, *Chem. Eng. J.*, 294 (2016) 290-297.
- [57] P. Khare, A. Yadav, J. Ramkumar, N. Verma, Microchannel-embedded metal-carbon-polymer nanocomposite as a novel support for chitosan for efficient removal of hexavalent chromium from water under dynamic conditions, *Chem. Eng. J.*, 293 (2016) 44-54.
- [58] J. Wang, P. Wang, H. Wang, J. Dong, W. Chen, X. Wang, S. Wang, T. Hayat, A. Alsaedi, X. Wang, Preparation of Molybdenum Disulfide Coated Mg/Al Layered Double Hydroxide Composites for Efficient Removal of Chromium(VI), *ACS Sustainable Chem. Eng.*, 5 (2017) 7165-7174.
- [59] M.K. Kim, K. Shanmuga Sundaram, G. Anantha Iyengar, K.-P. Lee, A novel chitosan functional gel included with multiwall carbon nanotube and substituted polyaniline as adsorbent for efficient removal of chromium ion, *Chem. Eng. J.*, 267 (2015) 51-64.
- [60] B.F. Abrahams, M.J. Grannas, L.J. McCormick, R. Robson, P.J. Thistlethwaite, Chiral and achiral linear coordination polymers from aldaric acids, *CrystEngComm*, 12 (2010) 2885-2895.
- [61] A. Lakatos, R. Bertani, T. Kiss, A. Venzo, M. Casarin, F. Benetollo, P. Ganis, D. Favretto, AlIII Ion Complexes of Saccharic Acid and Mucic Acid: A Solution and Solid-State Study, *Chem. Eur. J.*, 10 (2004) 1281-1290.
- [62] H.-Y. Zhang, G.-J. Zhang, X. Wang, J. Yang, X.-L. Chi, J.-L. Zhang, Y. Chen, Q. Yang, D.-R. Xiao, An unusual three-dimensional homochiral metal saccharate based on inorganic helical chains, *Inorg. Chem. Commun.*, 56 (2015) 73-75.
- [63] S.P. Kaiwar, C.P. Rao, In vitro reduction of Cr(VI) by low molecular weight biomimetic components: a comparative study using UV-Vis spectroscopy, *Chem.-Biol. Interact.*, 95 (1995) 89-96.
- [64] I. Kabdaşlı, T. Arslan, T. Ölmez-Hancı, I. Arslan-Alaton, O. Tünay, Complexing agent and heavy metal removals from metal plating effluent by electrocoagulation with stainless steel electrodes, *J. Hazard. Mater.*, 165 (2009) 838-845.

**Graphical abstract**

ACCEPTED MANUSCRIPT